8-17-2009

Single molecule force spectroscopy on g-quadruplex DNA

Susanna Lynch
Calvin University

Heather Baker
Calvin University

Sarah G. Byker
Calvin University

Dejian Zhou
University of Leeds

DOI: 10.1002/chem.200901390

Single Molecule Force Spectroscopy on G-Quadruplex DNA

Susanna Lynch,[a] Heather Baker,[a] Sarah G. Byker,[a] Dejian Zhou,*[b] and Kumar Sinniah*[a]

The interest in guanine (G) quadruplexes[1] has intensified over the past decade because they are found in human telomeres,[2] that is, the chromosome ends that govern gene stability, and other parts of the genome, especially in promoters.[3] They have been shown to inhibit the activity of telomerase, an enzyme which maintains the proper length of telomere DNAs and is overexpressed in many types of cancer.[4] As such, the G-quadruplex DNA has been an attractive target for cancer therapy.[5] Despite the wide interest in the topology of G-quadruplexes, their physical properties are not well-understood.[6] There are large differences between the kinetic data obtained in solution using fluorescence and on surfaces using surface plasmon resonance (SPR) approaches,[7] possibly due to destabilization by fluorophore labelling[7a–c] and surface hindrance in the indirect hybridization-based SPR approach.[7d] The kinetics and thermodynamics are expected to be different for G-quadruplexes formed from uni-, bi-, and tetramolecular DNA strands. Furthermore, G-quadruplexes formed from a single DNA strand may have different conformations,[6,7] where minor changes in the DNA sequence may result in significant differences in their thermodynamic properties.[6]

By taking measurements directly from unlabelled individual single molecules one at a time, thus avoiding measurement averaging, single-molecule (SM) force spectroscopy (FS) based on atomic force microscopy (AFM) has been demonstrated as a powerful tool to gain insights into a wide range of biological problems: protein folding,[8] protein–ligand interactions,[9] and DNA base-pairing.[10] Given the large number of G-quadruplex topologies possible,[1,2] SM-FS can potentially provide unique insights into their structure, function, and stability. Further, the recent development of theoretical analysis for SM approaches has enabled reliable estimates of the kinetic and thermodynamic parameters.[11] To the best of our knowledge, the AFM SM-FS has not been used to study G-quadruplex.[12] Herein, we present the first AFM based SM-FS study on a bi-molecular G-quadruplex system.

We used a bimolecular G-quadruplex formed between the AFM probe and a gold surface as the model system in this SM-FS study (see Figure 1). The DNA sequences and their abbreviations are given in Table 1. To perform the SM-FS study, a gold-coated Si_3N_4 probe and a flat gold surface were functionalized with a self-assembled monolayer (SAM) of the 3G or 4G DNA,[13] each having two G-rich domains, diluted by the spacer DNA at a ratio of 1:5.[13] Such dilution greatly reduces the possibility for the 3G/4G DNAs from forming intra-surface quadruplexes,[13d] while ensuring the forming of an inter-surface G-quadruplex when the probe and surface are brought into close proximity, and the observation of specific G-quadruplex SM rupture events when they are pulled apart. A representative force–distance curve for the 4G/3G DNAs is shown in Figure 1, which highlights an adhesion event followed by a stretching and the rupture of the G-quadruplex formed between the AFM probe and the surface.

To confirm the observed rupture event was due to an inter-surface quadruplex, two control experiments were carried out. The first used only the spacer DNA strand (A10) and the second used the 3G/4G mismatch DNAs diluted by the spacer DNA in the same ratio as those used for the 3G/4G DNAs. The mismatch DNAs have identical base constitutions to their respective 3G/4G DNAs, but the Gs are arranged differently to prevent them from forming bimolecular G-quadruplexes. The observed specific rupture events for 3G/4G quadruplexes is ~10% of the total force curves

[a] S. Lynch, H. Baker, S. G. Byker, Prof. K. Sinniah
Chemistry & Biochemistry, Calvin College
1726 Knollcrest Circle SE
Grand Rapids, MI 49546 (USA)
Fax: (+1) 616-526-6501
E-mail: ksinniah@calvin.edu

[b] Dr. D. Zhou
School of Chemistry and Astbury Center for
Structural Molecular Biology, University of Leeds
Leeds, LS2 9JT (UK)
Fax: (+44) 113-343-6565
E-mail: d.zhou@leeds.ac.uk

Supporting information for this article is available on the WWW under http://dx.doi.org/10.1002/chem.200901390.

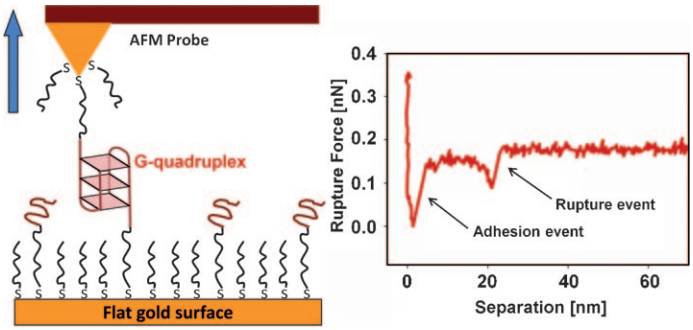

Figure 1. Left: Schematic diagram of the AFM SM-FS study on the G-quadruplex formation. Gold-coated AFM probe and surface are coated with a SAM of a thiolated 3G or 4G DNA, where each contains two G-rich domains (colored in brown) and an A_{12} spacer sequence (black), diluted by the spacer-DNA (A_{10}) at 1:5 molar ratio. An inter-surface quadruplex is formed between the probe and surface. Right: A typical force-distance curve obtained from the unbinding of an inter-surface G-quadruplex.

Table 1. DNA sequences (5′→3′) employed in this study. All DNAs are modified with a HS-$(CH_2)_6$ at 5′.

DNA	Sequence
3G	$(A)_{12}$-GGG TTA GGG
4G	$(A)_{12}$-GGG GAA TGG GG
3G mismatch	$(A)_{10}$-GAG TGT GAG AG
4G mismatch	$(A)_{10}$-GAG AGG AGG AGT G
spacer DNA	$(A)_{10}$

collected, while the 3G and 4G mismatch sequences showed <1 and $<0.1\,\%$, respectively, confirming that the observed rupture events are specific for the 3G/4G DNAs and resulted from the rupture of an inter-surface G-quadruplex. The mean rupture forces for the 3G and 4G DNAs were 49 ± 2 and 53 ± 3 pN, respectively, at a pulling speed of 198 nm s^{-1} in 100 mM K^+ Tris buffer (10 mM Tris·HCl, pH 7.4, see Supporting Information, Figure S1, for details). The rupture forces for the 3G and 4G quadruplexes are therefore almost identical, suggesting they have very similar mechanical resistance to mechanical unfolding. These values are greater than those for a unimolecular G-quadruplex obtained from optical tweezers unfolding, where ~23 and ~37 pN are reported for the parallel and anti-parallel G-quadruplexes.[12] The differences appear to be due to the different loading rates; a very low loading rate of 5.5 pN s^{-1} was used in the optical tweezers experiment,[12] whereas a much higher apparent loading rate of ~2000 pN s^{-1} was used here. The apparent loading rate has been found to have a significant impact on the rupture force for the bimolecular G-quadruplex system (see Figure 3).

Monovalent cations, for example, K^+ and Na^+, are involved in G-quadruplex formation and hence are important for G-quadruplex stability.[1,6,14] To investigate how K^+ concentration affects such inter-surface quadruplex mechanical stability, a K^+ titration study was performed with the 4G DNA, and the result is shown in Figure 2. A linear dependency of the mean rupture force on the K^+ concentration is observed (Figure 2), suggesting that these bimolecular G-quadruplexes formed at higher K^+ concentrations are more resistant to force-induced mechanical unfolding. This reveals for the first time that the mechanical strength of G-quadruplex is dependent on K^+ concentration, which correlates with earlier ensemble measurements that showed the melting temperature (TM) (i.e., thermodynamic stability) of unimolecular quadruplex increased with K^+ concentration.[14]

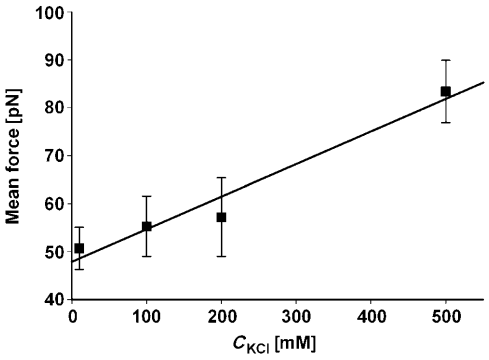

Figure 2. Plot of the mean rupture force (■) vs K^+ concentration for the bimolecular G-quadruplex DNA (4G). Force measurements were performed at a fixed apparent loading rate of 2000 pN s^{-1} in K^+ Tris buffer (10 mM Tris·HCl, pH 7.4); linear fit: ——, $R^2 = 0.9608$.

To estimate kinetic and thermodynamic parameters of the 3G and 4G quadruplexes, a loading rate dependence study was performed. Rupture forces were measured at apparent loading rates from 1027–43 500 pN s^{-1}. The force constant in AFM-based SM-FS approaches is much greater than that of the optical tweezers, allowing access to a greater range of force loading rates for probing energy barriers in biological systems. For each apparent loading rate, density plots were produced to obtain the most probable rupture force arising from a single quadruplex unbinding event. A plot of the rupture force as a function of the logarithm of the apparent loading rate is shown in Figure 3. The dependence of rupture force on the log (apparent loading rate) was analyzed by the recent theoretical models of Dudko–Hummer, assuming a single energy barrier[11] and the Bell–Evans model.[15] The solid lines in Figure 3 are theoretical fits to a linear cubic potential model ($\nu=2/3$) and a cusp potential model ($\nu=1/2$). These models provide independent estimates for the dissociation rate constant (k_0), barrier width ($x^{\ddagger}$), and free energy ($\Delta G^{\ddagger}$) from the unfolding of the quadruplex. The initial kinetic and thermodynamic estimates from the loading rate dependency plot were used to fit force distribution histograms. Each of the parameters was optimized, and the resulting theoretical force distribution is shown in Figures S3 and S4 in Supporting Information. The resulting best-fit kinetic and thermodynamic parameters are summarized in Table 2. For comparison, the kinetic off-rate (k_0) and barrier-width estimates using the phenomenological single-barrier Bell–Evans model[15] are also provided in Table 2 under $\nu=1$ for both 3G/4G quadruplexes. We have also attempted

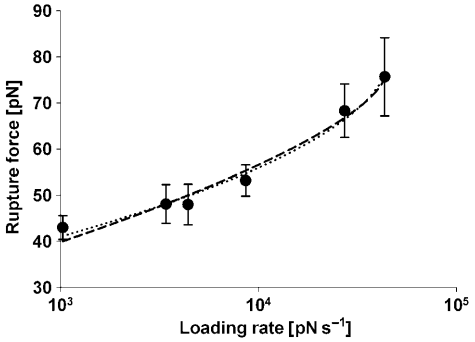

Figure 3. Dynamic force spectrum for the 4G quadruplex system at 100 mM K^+ in Tris (10 mM Tris·HCl, pH 7.4). Each data point on the graph refers to the most probable rupture force, which is the peak force obtained from a density function plot by a Gaussian fit. The apparent loading rate dependency data were modelled by cusp potential model ($\nu = 1/2$, •••••) and linear cubic potential model ($\nu = 2/3$, -----).

to fit the data with the two-barrier Bell–Evans model and the resulting fitting graphs and parameters are given in Figure S5 and Table S2 in Supporting Information.

Table 2. Kinetic and thermodynamic parameters for the 3G and 4G quadruplexes in 100 mM K^+ in Tris buffer (10 mM Tris·HCl, pH7.4).

	ν	$\Delta G^{\neq}$ [kcal mol^{-1}]	$x^{\neq}$ [nm]	k_0 [s^{-1}]
3G	1/2	4.3 ± 0.5	0.45 ± 0.05	1.65 ± 0.40
	2/3	4.1 ± 0.3	0.40 ± 0.05	1.50 ± 0.60
	1	–	0.26 ± 0.13	5.5 ± 2.6
4G	1/2	5.7 ± 0.1	0.85 ± 0.05	0.20 ± 0.05
	2/3	5.0 ± 0.3	0.70 ± 0.05	0.35 ± 0.10
	1	–	0.45 ± 0.05	1.6 ± 0.2

It is clear from Figure 3 that the rupture force for the G-quadruplex is loading rate dependent and increases non-linearly with increasing loading rate. The 4G quadruplex appears to be more thermodynamically stable (with a greater energy barrier $\Delta G^{\neq}$ to dissociation/unfolding) than the 3G quadruplex and dissociates more slowly. The k_0 value (off rate) for the 4G quadruplex is almost an order of magnitude smaller than the 3G quadruplex, despite having similar rupture forces. However, the differences in k_0 values between the 3G and 4G quadruplexes actually match very well with what was expected from their thermodynamic stability differences ($\Delta G^{\neq}$) (see Supporting Information for a detailed estimation). Furthermore, the k_0 for the bimolecular 4G G-quadruplex agrees extremely well with that of the unimolecular G-quadruplex (also containing four Gs in each G-rich stretch) obtained from the recent optical tweezers study.[12] We note, however, that this k_0 value is an order of a magnitude greater than the k_1 estimated by the two-barrier Bell–Evans model (see Table S2).

In summary, we have presented the first AFM-based SM-FS study on a bimolecular G-quadruplex system. This study shows that 3G and 4G quadruplexes have very similar resistance to force-induced mechanical unfolding (i.e., the number of G bases in each G-rich stretch does not have a significant impact on their mechanical stability) despite significant differences in the thermodynamic stability and folding off-rate. Their resistance to mechanical unfolding has been found to be strongly dependent on K^+ concentration. All these demonstrate that the AFM SM-FS is very powerful in probing the structure, kinetics, mechanical and thermodynamic properties of the G-quadruplex systems. Currently, we are investigating how G-quadruplex binding ligands, for example, insulin and drug molecules, affect the mechanical and thermodynamic properties of G-quadruplex. Given that G-quadruplexes are attractive targets for cancer therapy,[5] this may lead to the development of the AFM SM-FS as a novel tool for screening potential cancer therapeutic reagents.

Experimental Section

Thiolated DNA was immobilized on ultra-flat gold surface and on gold-coated AFM cantilever probe following our earlier established procedures[10c,13] and are described in detail in the Supporting Information. All force spectroscopy measurements were performed using a Picoforce AFM (Veeco Metrology, California, USA). Spring constants of cantilevers were measured using the thermal fluctuation method and ranged from 33–54 pN nm^{-1}. For dynamic force measurements, a contact force of 200 pN, ramp size of 250 nm, and surface delay of 1 s was used. The apparent loading rate was obtained for each force curve by taking the product of the slope prior to rupture and the pulling velocity. For a fixed pulling velocity, the apparent loading rate reported is the median apparent loading rate obtained from the analysis of ~100 force distance curves. Details of the experimental procedures, data analysis and supporting figures are available in the Supporting Information.

Acknowledgements

This work was supported by the National Institutes of Health (Grant 1R15GM073662-01) and a Calvin College Alumni Grant. We thank Prof. Olga Dudko (UCSD) for helpful discussions and suggestions.

Keywords: atomic force microscopy · DNA · G-quadruplex · single-molecule studies

[1] a) S. Neidle, S. Balasubramanian in *Quadruplex Nucleic Acids*, RSC, Cambridge, **2006**; b) P. Bates, J.-L. Mergny, D. Yang, *EMBO Rep.* **2007**, *8*, 1003–1010.

[2] a) J. T. Davis, *Angew. Chem.* **2004**, *116*, 684–716; *Angew. Chem. Int. Ed.* **2004**, *43*, 668–698; b) J-L. Mergny, J.-F. Riou, P. Mailliet, M. P. Teulade-Fichou, E. Gilson, *Nucleic Acids Res.* **2002**, *30*, 839–865; c) S. Neidle, G. Parkinson, *Nat. Rev. Drug Discovery* **2002**, *1*, 383–393.

[3] a) J. L. Huppert, S. Balasubramanian, *Nucleic Acids Res.* **2005**, *33*, 2908–2916; b) J. L. Huppert, S. Balasubramanian, *Nucleic Acids Res.* **2006**, *35*, 406–413.

[4] a) J.-F. Riou, D. Gomez, H. Morjani, C. Trentesaux in *Quadruplex Nucleic Acids* (Eds.: S. Neidle, S. Balasubramanian), RSC, Cambridge, **2006**; b) F. Lavelle, J-F. Riou, A. Laoui, P. Mailliet, *Crit. Rev. Oncol. Hematol.* **2000**, *34*, 111–126.

[5] a) S. Neidle, G. N. Parkinson, *Biochimie* **2008**, *90*, 1184–1196; b) N. H. Campbell, G. N. Parkinson, A. P. Reszka, S. Neidle, *J. Am.*

Chem. Soc. **2008**, *130*, 6722–6724; c) L. H. Hurley, *Nat. Rev. Cancer* **2002**, *2*, 188–200.

[6] A. N. Lane, J. B. Chaires, R. D. Gray, J. O. Trent, *Nucleic Acids Res.* **2008**, *36*, 5482–5515, and references therein.

[7] a) L. Ying, J. J. Green, H. Li, D. Klenerman, S. Balasubramanian, *Proc. Natl. Acad. Sci. USA* **2003**, *100*, 14629–14634; b) J. J. Green, L. Ying, D. Klenerman, S. Balasubramanian, *J. Am. Chem. Soc.* **2003**, *125*, 3763–3767; c) S. S. White, S. Balasubramanian, D. Klenerman, L. Ying, *Angew. Chem.* **2006**, *118*, 7702–7705; *Angew. Chem. Int. Ed.* **2006**, *45*, 7540–7543; d) Y. Zhao, Z. Y. Kan, Z. X. Zeng, Y. H. Hao, H. Chen, Z. Tan, *J. Am. Chem. Soc.* **2004**, *126*, 13255–13264.

[8] A. Borgia, P. M. Williams, J. Clarke, *Annu. Rev. Biochem.* **2008**, *77*, 101–125, and references therein.

[9] a) D. J. Müller, Y. F. Dufrene, *Nat. Nanotechnol.* **2008**, *3*, 261–269; b) D. J. Muller, *Biochemistry* **2008**, *47*, 7986–7998; c) K. C. Neuman, A. Nagy, *Nat. Methods* **2008**, *5*, 491–505; d) C. K. Lee, Y. M. Wang, L. S. Huang, S. Lin, *Micron* **2007**, *38*, 446–461; e) L. Porter-Peden, S. Kamper, M. Vander Wal, R. Blankespoor, K. Sinniah, *Langmuir* **2008**, *24*, 11556–11561; f) S. G. Kamper, L. Porter-Peden, R. Blankespoor, K. Sinniah, D. J. Zhou, C. Abell, T. Rayment, *Langmuir* **2007**, *23*, 12561–12565; g) X. Wang, D. J. Zhou, K. Sinniah, C. Clarke, L. Birch, H. Li, T. Rayment, C. Abell, *Langmuir* **2006**, *22*, 887–892.

[10] a) T. Strunz, K. Oroszlan, R. Schafer, H. J. Guntherodt, *Proc. Natl. Acad. Sci. USA* **1999**, *96*, 11277–11282; b) L. H. Pope, M. C. Davies, C. A. Laughton, C. J. Roberts, S. J. B. Tendler, P. M. Williams, *Eur. Biophys. J.* **2001**, *30*, 53–62; c) M. Vander Wal, S. Kamper, J. Headley, K. Sinniah, *Langmuir* **2006**, *22*, 882–886.

[11] a) O. K. Dudko, J. Mathe, A. Szabo, A. Meller, G. Hummer, *Biophys. J.* **2007**, *92*, 4188–4195; b) O. K. Dudko, G. Hummer, A. Szabo, *Proc. Natl. Acad. Sci. USA* **2008**, *105*, 15755–15760.

[12] Z. Yu, J. D. Schonhoft, S. Dhakal, R. Bajracharya, R. Hegde, S. Basu, H. Mao, *J. Am. Chem. Soc.* **2009**, *131*, 1876–1882.

[13] a) D. J. Zhou, K. Sinniah, C. Abell, T. Rayment, *Angew. Chem.* **2003**, *115*, 5084–5087; *Angew. Chem. Int. Ed.* **2003**, *42*, 4934–4937; b) D. J. Zhou, K. Sinniah, C. Abell, T. Rayment, *Langmuir* **2002**, *18*, 8278–8281; c) D. S. Liu, A. Bruckbauer, C. Abell, S. Balasubramanian, D. J. Kang, D. Klenerman, D. J. Zhou, *J. Am. Chem. Soc.* **2006**, *128*, 2067–2071; d) W. Wang, H. Liu, D. Liu, Y. Xu, Y. Yang, D. J. Zhou, *Langmuir* **2007**, *23*, 11956–11959; e) D. Zhou, A. Bruckbauer, L. M. Ying, C. Abell, D. Klenerman, *Nano Lett.* **2003**, *3*, 1517–1520.

[14] N. V. Hud, J. Plavec in *Quadruplex Nucleic Acids* (Eds.: S. Neidle, S. Balasubramanian), RSC, Cambridge, **2006**, p. 100.

[15] a) E. Evans, *Annu. Rev. Biophys. Biomol. Struct.* **2001**, *30*, 105–128; b) E. Evans, *Faraday Discuss.* **1999**, *111*, 1–16.

Received: May 25, 2009
Published online: July 14, 2009

